Increased Stream Temperature in Response

to Extreme Precipitation Events

by

Colleen E. Wilson

B.S., University of Maryland, 2015

A thesis submitted to the

Faculty of the Graduate School of the

University of Colorado in partial fulfillment

of the requirements for the degree of

Master of Science

Department of Civil, Environmental, and Architectural Engineering

2017

This thesis entitled:

Increased Stream Temperature in Response to Extreme Precipitation Events

Written by Colleen E. Wilson

Has been approved for the Department of Civil, Environmental and Architectural Engineering

_____

Michael Gooseff

_____

Ben Livneh

_____

Roseanna Neupauer

Date _____

The final copy of this thesis has been examined by the signatories, and we find that both the content and the form meet acceptable presentation standards of scholarly work in the above mentioned discipline.

Colleen E. Wilson (M.S., Civil Engineering)

Increased Stream Temperature in Response to Extreme Precipitation Events

Thesis directed by Dr. Michael N. Gooseff

Aquatic ecosystem temperature regulation is essential to the survival of riverine fish species restricted to limited water temperature ranges. Thermal effluent regulations in place to protect these ecosystems restrict thermoelectric power generation when water temperatures are too warm. Climate change projections forecast increased precipitation intensities, a trend that has already been observed in the past century. Though extreme events are becoming more common, the stream temperature response to high-intensity rainfall is not yet well understood. Precipitation (33) and stream temperature records (52) from gages in the Upper Midwestern United States were analyzed to determine whether there exists a positive relationship between high-intensity rainfall and warming stream temperature response. This region was chosen for its already observed trends in increasing precipitation intensity, and both urban and rural gages were used in order to account for the effect of impervious surfaces on runoff amounts and temperature. Days with recorded precipitation were divided by an intensity threshold and classified as either high-intensity or moderate-intensity days. While the effects of rain events on stream temperature are variable, increases in stream temperature in response to high-intensity rainfall were observed. For some basins, daily maximum rates of stream temperature increase were, on average, greater for higher intensity events. Similarly, the daily maximum rate of temperature increase was higher in most streams on days of high-intensity precipitation, compared to days of moderate-intensity events. Understanding the effect of increasing precipitation intensity in conjunction with rising air temperatures will provide insight into the future of aquatic ecosystems and their adaptation to climate change.

Dedication

To my grandfather, Joe Smith, who always enthusiastically supported every crazy idea that ever popped into my head.

Acknowledgements

My brilliant advisor, Mike Gooseff for his guidance

My wonderful committee, Ben Livneh and Roseanna Neupauer

Joe Kasprzyk for his instrumental help in the organizational and writing processes

Kent Mills, for his knowledge of nuclear power plant operations

The Gooseff Research Group, especially Anna Bergstrom, Maggie Spangler, and Adam Wlostowski for their invaluable input, suggestions, and friendship

Matt Alongi and Tim Clarkin, for helping me navigate through the thesis writing process

Billy Raseman, for lunchtime running breaks and helping with all things statistics

Gillian Asque, for helping me decipher water law

The rest of my cohort of classmates: Elliot Alexander, Maggie McHugh, Mickey Rush, and Jenna Stewart, for homework help, camaraderie, and general shenanigans

Shaun Carney, Katie Ordal, and Jon Quebbeman at RTI for their flexibility and encouragement as I balanced work and school

The Boulder Women's Running Group, especially Sylvie Frank, Trea Nance, and Sarah Wilson, for giving me an excuse to get outside and stretch my legs

Abby Ahlert, for moving from Maryland to Colorado with me in the first place

My siblings: Claire, Dan, Emily, and Ally, for encouraging me to do my own thing

And of course, my parents, for their unconditional love and support

Table of Contents

List of Figures

List of Tables

1. Introduction

1.1 Changing Precipitation Intensity in the United States

The continental United States has seen an observed increase in the frequency of extreme precipitation events. Traditional hydrology allows the assumption of stationarity in the statistical calculation of rainfall amounts for specified return periods and storm durations. However, studies from the 1980's onward have shown that this may not be true (Milly et al., 2008; Angel and Huff, 1997). A widespread increase in the upper 10th percentile of the precipitation distribution for the contiguous United States has been documented (Karl and Knight, 1998), noting an overall 10% increase in precipitation amount, with 53% of the total increase attributable to positive trends in the upper 10th percentile of the precipitation distribution. In a study of the precipitation record from 1893-2002, Groisman et al. (2004) observed a 20% increase in very heavy precipitation for the United States. The 20% observed increase occurred entirely during the last third of the 20th century. A study of 304 Midwestern sites with records from 1901-1994 found a statistically significant positive trend in the number of extreme precipitation events (Angel and Huff, 1997). Villarini et al. (2013) similarly observed increasing trends over the northern Midwest. A comparison with the surface air temperature record suggested that increasing rainfall intensity trends occur over areas with the largest increasing trends in temperature. Warmer air temperature results in an increase in water vapor, thus fueling increases in precipitation.

As an increase in precipitation intensity has been observed, so has an increase in air temperature. 18% of moderate precipitation extremes occurring worldwide can be attributed to warming air temperatures (Rischer and Knutti, 2015). Freshwater stream

temperature variability is already regulated by atmospheric air temperature (e.g. Sinokrot et al., 1994; Constanz, 1998; Caissie, 2006; Kelleher et al., 2012). The purpose of this study is to determine the impact of increased precipitation intensity on stream temperature.

1.2 Traditional Hydrology

1.2.1 Sources of Streamflow

When water in the atmosphere precipitates, it can discharge as surface runoff or infiltrate the soil. After infiltration, it can become subsurface flow (interflow), or, if it infiltrates deep enough, it can recharge the groundwater. During dry periods, streams are generally fed by groundwater, as seen in Figure 1a. During precipitation events, streams can be fed by groundwater still, but additional sources of streamflow include overland flow and interflow, as seen in Figure 1b (Mays, 2011).

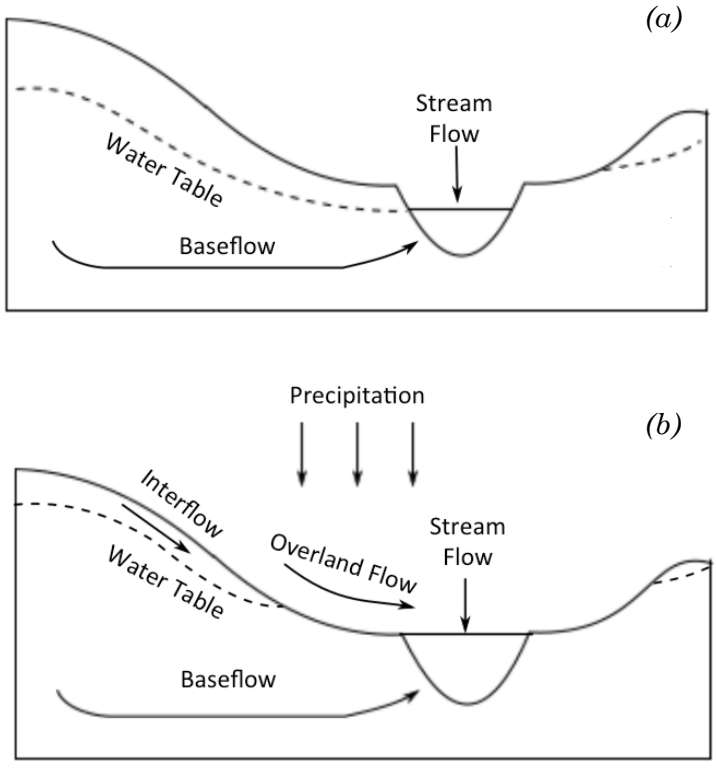

Figure 1: (a) Sources of streamflow during a dry period (b) Sources of streamflow during a rain event (adapted from Mosley and McKerchar, 1993)

1.2.2 Factors Affecting Stream Temperature

Traditionally understood to affect stream temperature are factors that are related to one of four different groups: atmospheric conditions, topography, stream discharge, and streambed (e.g., Caissie, 2006). With respect to atmospheric conditions, for example, stream temperature is affected by the amount and rate of absorption and irradiation of solar heat as well as by evaporation by sun and wind. With topography, the shape of the channel affects temperature through the amount of water surface exposed to air and sunlight, and discharge has an impact because the larger the volume of flow, the slower the change in temperature. Below the surface, temperature and volume of groundwater inflow can change the temperature as well (Blakey, 1966).

At its source, stream water temperature is normally close to groundwater temperature (Caissie, 2006). As water moves downstream, unregulated streams are controlled mainly by atmospheric conditions, with streambed fluxes accounting for less than -0.12 to +0.15°C (-0.22 to +0.27°F) in terms of water temperature variability (Sinokort et al., 1994). In a study by Evans et al. (1998), on average, about 72% of the variation in stream water temperature was attributed to air temperature and incoming shortwave radiation. Water temperature in streams generally is at its minimum around sunrise, which is also the average time of minimum air temperature, and it peaks in the late afternoon to early evening, as with air temperature. Heat exchange at the air/water interface is a result of net incoming solar short-wave radiation, net outgoing long-wave radiation, evaporative heat flux, convective heat transfer, and relatively small contributions form precipitation and friction (Caissie, 2006).

As noted above, upwelling groundwater temperature is often assumed to be equal to mean annual air temperature. For some catchments, discharge to the stream is dominated not by the inflow of deeper groundwater, but by shallow subsurface flow. These catchments

are characterized by more variable temperatures variations than deep-groundwater dominated catchments (Leach and Moore, 2014).

Most frequently, when rain falls onto a permeable surface, it infiltrates the soil pushes groundwater into the stream. Traditionally in the field of hydrology, groundwater is assumed to be equal to mean annual surface air temperature plus a potential thermal offset of up to 3°C (5.4°F) (e.g. Ficklin, 2012 and MacDonald, 2014). Therefore, in the winter, groundwater temperature is usually warmer than the surface, and in the summer, it is cooler. If, during a summer rain event, infiltrating rainwater pushes groundwater into the stream channel, the temperature should be expected to decrease, as shown in Figure 2a. However, if extreme rainfall intensity causes the soil to reach its infiltration capacity, it could cause an increase in surface runoff, as seen in Figure 2b. Since rainwater can be roughly assumed to be equal to air temperature, which is generally warmer than stream temperature in the summer, and increase in surface runoff would result in an expected increase in stream temperature (e.g. Nelson and Palmer, 2007). This study attempts to answer the following question: if precipitation intensity increases, will there be a corresponding increase in stream temperature?

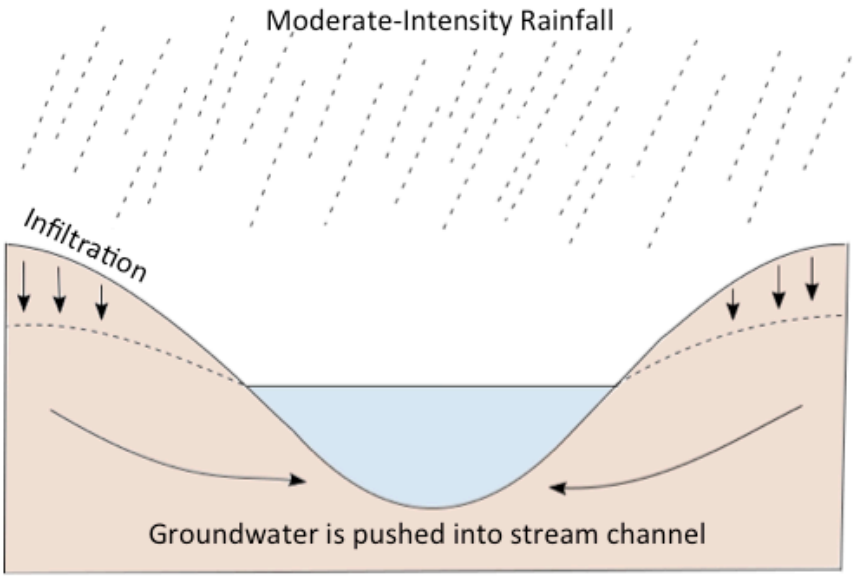

(a)

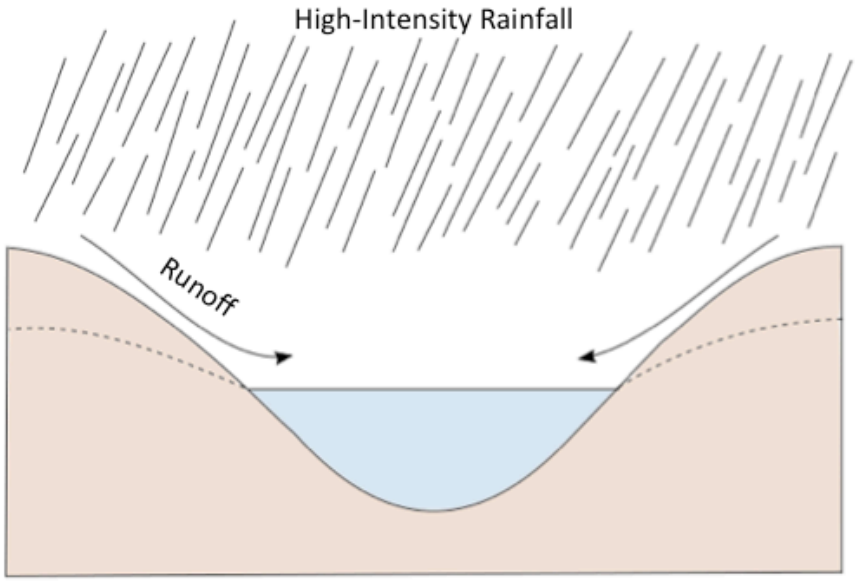

(b)

Figure 2: (a) Schematic of a moderate-intensity rainfall event. Moderate-intensity rainfall infiltrates soil and pushes relatively colder groundwater into the stream channel, lowering stream temperature. (b) High-intensity rainfall cannot infiltrate soil and instead relatively warmer water runs off into the stream channel, raising stream temperature.

1.3 Motivation

From the ecology to economics, the impact of stream temperature can be observed. In our analysis, we will examine the impact of stream temperature in conjunction with fisheries and overall ecological river health, thermoelectric power generation, and the current laws in place that govern stream temperatures.

1.3.1 Stream Ecology

Fish can only survive in restrictive temperature ranges (e.g. Eaton and Scheller, 1996; Torgerson et al., 1999; and Caissie, 2006;). Hence, fish populations are at risk of shrinking with increased water temperatures. According to the American Sportfishing Association, recreational fishing generates more than $125 billion in overall economic output, $16.4 billion in tax revenue, and more than one million jobs (Allen and Southwick, 2008). This economic activity could be impacted if stream temperature increases past a threshold for which fish can no longer thrive.

The temperature for which death is imminent, known as the critical thermal maxima, ranges from 90-104°F. Historically, fish deaths due to extremely warm water temperatures are rare. High temperatures generally induce frantic activity in fish, which encourages them to flee in search of cooler waters (Beitinger et al., 2000). Torgersen et al., (1999), for example, observed that Chinook salmon in northeastern Oregon thermoregulate by moving to cooler areas, such as confluences with cold streams, when water temperatures exceed their upper tolerances. However, if stream waters warm, thermal refugia may become harder for fish to find. Eaton and Scheller (1999) used a climate model to project the increase in water temperatures associated with a doubling of CO_2. Their results indicated that the habitat for cold and cool water fish would be reduced by about 50%. Habitat losses would be greatest for species with the smallest initial distributions and in geographic regions with the greatest warming, such as the central Midwest.

Temperature also affects the amount of oxygen that water can hold. The saturation value for dissolved oxygen in water is 14 ppm at 34°F, and drops to less than 8 ppm at 80°F (Blakey, 1966). Oxygen availability is essential for overall ecosystem health. Decreases in dissolved oxygen can result in changes in fish behavior and survival rates (Schlosser, 1991).

1.3.2 Thermoelectric Power Generation

In the United States, 91% of total electricity is produced by thermoelectric (i.e. nuclear and fossil-fuelled) power plants. These power-generating systems rely heavily on the availability and temperature of river waters for cooling. At 40% of total surface water withdrawals, thermoelectric power is one of the largest water users in the U.S. Individual power plants must meet regulations for the temperature of water they can release back to the river system. If water temperatures are too warm at intake, the power plant may be forced to halt operations (Van Vliet et al., 2012). Peak electricity demands are higher than average during warm weather because of the energy needed for air conditioning. However, due to temperature regulations, less electricity can be produced when water temperatures are too high (Van Vliet et al., 2016). Some power plants take measures to reduce the temperature of water that is released back into the river. One such method is the use of cooling towers, but the cooling process results in evaporation loss, which means less water is discharged than is taken in. To avoid loss to evaporation, a second tactic to lower the temperature of effluent is the use of condensers. Condensers both minimize withdrawal losses and reduce heat loads, but the amount of energy required to accomplish these objectives results in a less efficient power-generating system overall. No matter the use of cooling towers or condensers, there is always a net increase in the stream temperature when it is used for thermoelectric cooling (Koch et al., 2009).

1.3.3 Temperature Regulations

In order to ensure overall ecosystem health in conjunction with thermal effluent from activities such as thermoelectric power generation, there exist laws at the federal and state levels. The Clean Water Act outlines the purpose for regulating water pollution, including thermal pollution. The Act also allocates funds and support for state governments (33 U.S.C. 26). The three states analyzed in this study have regulations for stream water temperature in their respective state administrative codes. The regulations differ slightly from state to state, but all have the common goal of fishery health. Temperature requirements for coldwater fisheries are especially stringent. A summary of the water temperature regulations with respect to coldwater fisheries can be found in Appendix A2.

2. Methods

This study is not a demonstration in how precipitation intensity is changing or how stream temperature is changing through time. Rather, this study used 21st century stream data to demonstrate the difference between the stream temperature responses to high intensity precipitation events compared to that of moderate intensity events.

2.1 Site Description

In order to examine the relationship between precipitation intensity and stream temperature, we chose to focus on the American Midwest for its documented observed increase in precipitation intensity. 52 U.S. Geological Survey (USGS) stream gages were chosen in Iowa, Wisconsin, and Michigan, which can be seen in Figure 3. Drainage areas ranged from 3.58 to 316,200 square miles. A complete list of the gages can be found in Appendix A1. These Midwestern states were chosen specifically for their abundance of available stream gages. Most Minnesota water data collection platforms, for example, were located in lakes. From the available gages in the three chosen states, gages with an obvious impact from dam regulation or power plant discharge were removed.

The region is classified through the Köppen Climate Classification as having a humid continental climate with relatively evenly distributed precipitation throughout the year. That is, the region does not have a distinction between dry and rainy seasons (Kottek et al., 2006). Sun and Lall (2015) developed a Bayesian model to identify clusters of stations with similar temporal patterns. The model found the Midwest to have spatially consistent trends in temporal patterns at the cluster and station level. Annual maximum daily rainfall exhibits a noticeable seasonality. The largest frequencies of heavy rainfall occur between May and August. There is a temporal clustering behavior of heavy rainfall

events regulated by climatic factors influenced by both the Atlantic and Pacific Oceans (Villarini et al., 2011).

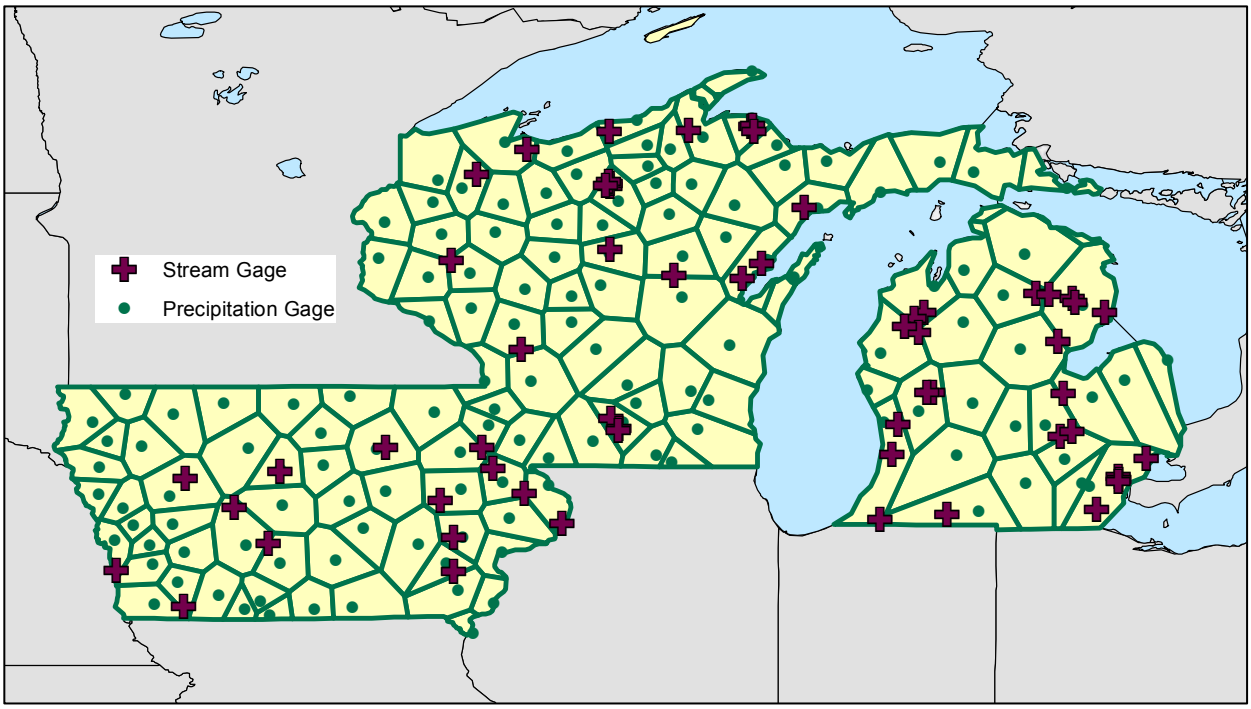

Figure 3: The study area containing Iowa, Wisconsin, and Michigan. USGS stream gages are maroon plus signs, and precipitation gages are green circles. Corresponding Thiessen polygons are outlined in green.

2.2 Stream and Precipitation Gage Selection

The selected 52 USGS stream gages had both 15-minute stream discharge and 15-minute temperature data. The period of record used for each of these gages went back no earlier than 2007. Precipitation data came from the National Oceanic and Atmospheric Administration (NOAA) National Centers for Environmental Information. Precipitation totals were sampled, like the stream gage data, on 15-minute intervals.

Each stream gage was assigned to a corresponding precipitation gage through the Thiessen polygon method (Thiessen, 1911). This method was demonstrated for use in precipitation gages for example, by Teegavarapu and Chandramoili (2005) and Fiedler (2003). Each precipitation gage is represented by a point, and surrounding each gage is a

polygon so that for any location within that polygon, the nearest precipitation gage is the gage at the center of the polygon. This method would not be very accurate for a mountainous region, as it does not take into account slopes or topographical divides, but for the relatively flat Midwest, it is an acceptable method for assigning precipitation gages to stream gages. These gages are included in Appendix A1.

2.3 Analysis of Drainage Area Conditions

For the region surrounding each stream gage, we analyzed the soil type, impervious surface area, and antecedent moisture. The region selected for examination was the Hydrologic Unit Code (HUC) Level 12 containing the stream gage.

2.3.1 Impervious Surface Area

For each HUC 12 surrounding each stream gage, we looked at the impervious surface area. Impervious surface area has been observed to have an effect on stream temperature because the rainwater is unable to infiltrate the soil when it hits impervious paved surfaces. If rainwater is able to infiltrate the soil, it can effectively displace the relatively cooler groundwater into the stream channel. If water cannot infiltrate, but rather hits the hot impervious surface, the precipitation joins the stream as warm runoff and increases the temperature of the stream. This effect has been studied extensively, especially with respect to urbanization (e.g. Nelson and Palmer, 2007; Somers et al., 2016). In a study of 1,485 summer days in Maryland, the proportion of monitored summer days with temperature surges ranged from 0% at an agricultural site to 10% at a highly urbanized site (Nelson and Palmer, 2007).

We measured the percent impervious surface area in order to determine whether differing stream temperature responses to high-intensity rainfall were simply a question of impervious surface area. We wanted to address the possibility that a warming response to high-intensity rainfall could occur independent of impervious surface area. The percent

impervious surface area was calculated for each HUC 12 containing a stream gage from the 2011 National Land Cover Database (NCLD 2011) using the Zonal Statistics as Table tool in ArcGIS. An example of the HUC 12 with impervious surface area is seen in Figure 4.

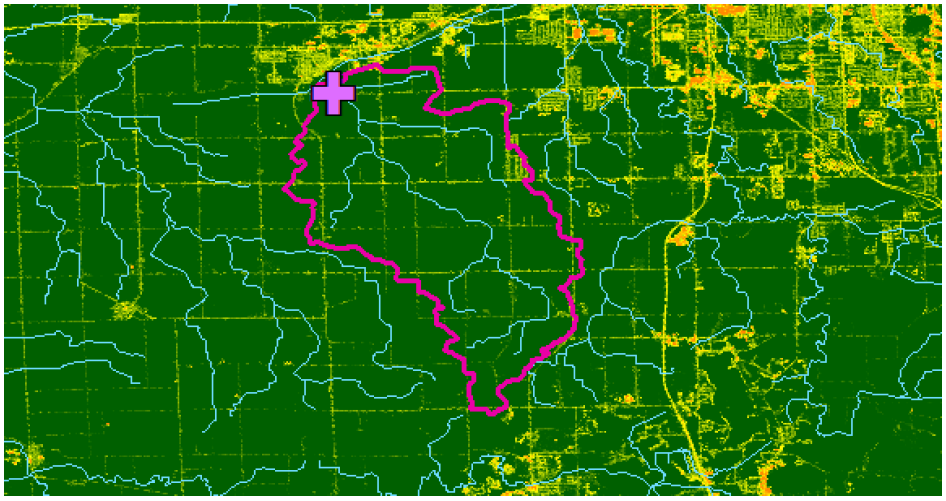

Figure 4: The HUC 12 area (outlined in pink) for USGS Gage at Alger Creek at Hill Road near Swartz Creek, MI (purple plus sign). Higher percentage impervious surfaces are warmer colors.

2.3.2 Hydrologic Soil Group

We compared the soil types for the catchment areas of the stream gages using the HUC 12 areas for both the unit containing the stream gage and the unit containing the precipitation gage. This analysis was completed in order to determine if there was any trend between soil type and heating response. NRCS hydrologic soil groups are defined by the Natural Resources Conservation Service (NRCS) and classified by their ability for water to infiltrate soil. They are a reflection of the soil's proclivity for runoff. Properties considered for soil group classification include depth to a restrictive layer or water table, transmission rate of water, texture, structure, and degree of swelling (Mays, 2011). Properties of the different soil groups are summarized in Table 1 (McCuen, 2004).

Table 1: Hydrologic Soil Groups

Group	Minimum infiltration rate (in/hr)	Runoff potential
A	0.30-0.45	Very low
B	0.15-0.30	Moderately low
C	0.05-0.15	Moderately high
D	0-0.05	Very high

2.3.3 Antecedent Moisture

In a final analysis of drainage area characteristics, by proxy, pre-storm antecedent soil moisture was determined for each rainfall day through the summation of total rainfall in the previous five days.

Precipitation records from NOAA are only publicly available through the end of 2013. So, only data for which the time period of record of both the stream gage and precipitation gage overlapped were used. Many of the rivers in the Midwest freeze during the winter. In order to focus solely rainfall and eliminate the effects of ice and snowfall, winter dates were also removed from the period of record used. Thus, only dates that fall on or between May 1 and September 30 were used.

2.4 Division of Data

2.4.1 Temporal Division of Data

The remaining data was divided by 24-hour periods from 6 am to 6 am. 6 am was chosen because stream temperature is generally at its minimum around sunrise (Maheu, et al., 2016). Dividing the days at 6 am allowed us to capture the full diurnal temperature cycle in one 24-hour period, which in broad patterns is explained by the diurnal variability in air temperature at the U.S. continental scale (Maheu et al., 2015). The 6am date

division also allowed the entirety of overnight thunderstorms to be contained within one period rather than be split at midnight between two different days.

2.4.2 Rainfall Intensity Classification

Once the data was divided into 24-hour periods, each day was classified as one of three types of days: high-intensity precipitation, moderate-intensity precipitation, or zero precipitation. A high-intensity day was defined as any date with at least one 15-minute time period above the high-intensity precipitation threshold. The threshold was calculated separately for each individual precipitation gage, by finding the 95th percentile of the distribution of non-zero 15-minute precipitation time periods. This method came from Groisman et al., (2004) who classified the upper 10-5% of the precipitation distribution as the threshold for "heavy precipitation." For most gages, the threshold was around 0.2 inches per 15-minute period (0.8 inches per hour). Days that had some measureable precipitation, but no 15-minute periods above the threshold were classified as moderate-intensity precipitation days, and days without any measureable precipitation were categorized as no precipitation days. These classifications are summarized in Table 2.

Table 2: Rainfall Intensity Classification

Intensity Classification	Maximum Observed Intensity
No precipitation	No precipitation observed
Moderate-intensity precipitation	0 - 95th percentile
High-intensity precipitation	>95th percentile

2.4.3 Classification of System Sensitivity to High-Intensity Rainfall

The difference between high and moderate intensity rainfall was examined by comparison of parameters related to discharge and temperature data. First, the daily maximum hourly change in temperature, dT/dt, where T is temperature and t is time, was

calculated. This was determined by using a moving hourly window through the temperature data to find the maximum positive change in temperature as demonstrated in Figure 5. Then, for each stream gage, all of the maximum daily hourly changes in temperature were averaged separately for each precipitation intensity classification: high-intensity, moderate-intensity, and no precipitation days.

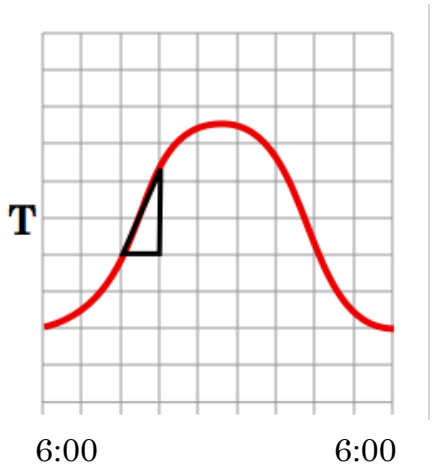

Figure 5: dT/dt measured as the maximum positive slope of the temperature variation. Time interval is one hour.

Gages that had a higher mean maximum hourly dT/dt for high-intensity rainfall days than for moderate-intensity rainfall days were classified as gages with a high-intensity rainfall sensitive response, henceforth referred to sensitive response (SR) systems. Gages where the mean maximum hourly dT/dt was higher for the moderate-intensity days were categorized as buffered response (BR) systems. Looking at the maximum hourly change in temperature served as a proxy for assuming the dominant flow of the system. We estimated SR systems to be dominated by overland flow, whereas BR systems were assumed to be groundwater flow dominated.

To summarize, the data was divided by high-intensity rainfall dT/dt response and daily precipitation threshold into the following six categories seen in Table 3:

Table 3: Data Classification Categories

Sensitive response (SR) gages	Buffered response (BR) gages
1. No precipitation	4. No precipitation
2. Moderate-intensity precipitation	5. Moderate-intensity precipitation
3. High-intensity precipitation	6. High intensity precipitation

2.5 Stream Parameters Evaluated

Each gage was then evaluated for the following six parameters related to stream discharge and temperature as seen in Table 4.

Table 4: Parameters Evaluated

Discharge, Q	Temperature, T
1. Daily maximum Q	4. Daily maximum T
2. Daily Q range	5. Daily T range
3. Daily maximum dQ/dt	6. Daily heat accumulation, η

2.5.1 Discharge

Daily maximum discharge (Q) was calculated by finding the absolute maximum instantaneous stream discharge for each 24-hour period, as seen in Figure 6a. The daily Q range is defined as the difference between the absolute daily maximum Q and absolute daily minimum Q for each 24-hour period, shown in Figure 6b. Daily maximum dQ/dt was calculated using a sliding one-hour window through the time period. Within the window, beginning of hour Q was subtracted from end of hour Q. The highest positive value was the daily maximum dQ/dt, as seen in Figure 6c.

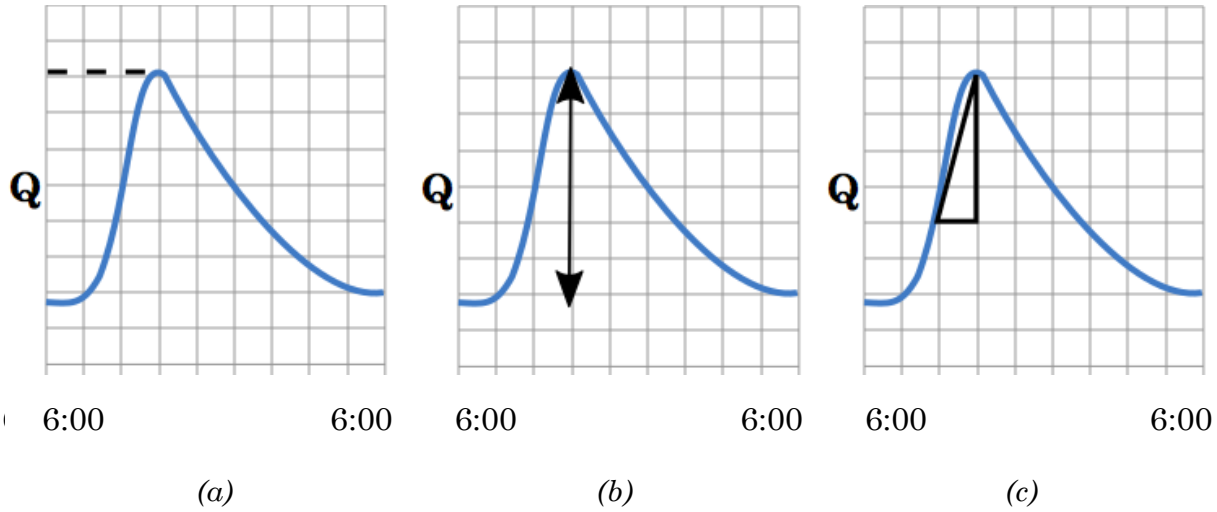

Figure 6: (a) Maximum Q measured as the maximum value on the hydrograph. (b) Q Range measured as the maximum value minus the minimum value. (c) Maximum dQ/dt calculated as the maximum change in discharge per hourly window.

2.5.2 Temperature

Daily maximum *T* was determined by a method similar to that of daily maximum *Q*. Daily maximum *T* is the absolute maximum instantaneous temperature reached during a 24-hour period, as seen in Figure 7a. Daily *T* range is defined as the difference between absolute maximum instantaneous temperature and absolute minimum instantaneous temperature, shown in Figure 7b. Daily heat accumulation, η, is defined as the total amount of heat experienced by a given stream gage above the threshold equal to the freezing point of water, 0°C. Heat accumulation is defined by the following integral equation:

$$\eta = \int_{t_1}^{t_2} T\, dt \qquad (1)$$

where t_1 is equal to 6:00 am on the current day, t_2 is equal to 6:00 am 24 hours later, and T is equal to instantaneous temperature in degrees Celsius above freezing, as shown in Figure 7c. The resulting heat accumulation is in units of degrees Celsius by 24-hours. This

method was inspired by the double triangle method for heat accumulation first defined by Sevacherian et al. (1977) and applied to stormwater heat pulse measurement by Somers et al. (2006).

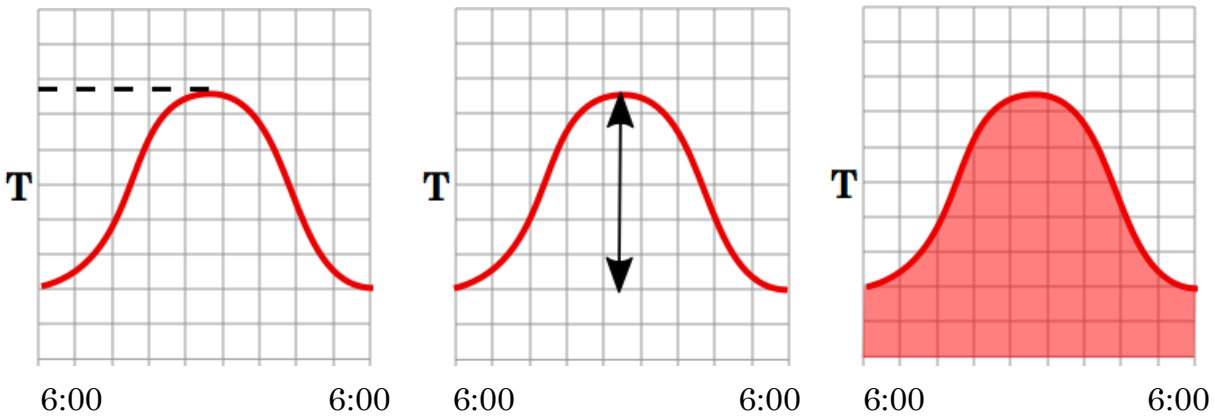

Figure 7: (a) Maximum T measured as the maximum value of the daily temperature variation. (b) T Range measured as the maximum value minus the minimum value. (c) Accumulated heat as measured as the area under the temperature curve and above 0°C

2.6 Antecedent Moisture

To assess the impact of pre-storm soil moisture on temperature response, we calculated antecedent moisture content on a given day as the total precipitation of the previous five days.

2.7 Application to Midwestern Trout Species

In order to analyze the ecological effect of stream temperature response to high-intensity rainfall, the range of daily maximum temperatures for each gage were compared to the preferred temperature range for two species of fish commonly found in Midwest streams. The Rainbow Trout (*Oncorhynchus mykiss*) and the Brook Trout (*Salvelinus fontinalis*) are both coldwater fish. Their temperature tolerances are summarized in Table 6. Preferred temperature refers to the range in which the species are most healthy.

Critical thermal maximum is the threshold above which the fish are likely to die (Beitinger et al., 2000).

Table 5: Trout Temperature Tolerances

Common name	Latin name	Preferred temp.	Critical thermal max.
Rainbow Trout	*Oncorhynchus mykiss*	53-57°F 12-14°C (Dehring, et al., 2008)	26.9°C (Becker and Wolford, 1980) to 29.8°C (Currie et al., 1998)
Brook Trout	*Salvelinus fontinalis*	53-57°F 12-14°C (Dehring and Krueger, 2008)	28.7-29.8°C (Lee and Rinne, 1980)

3. Results

3.1 Case Study: East Branch Salmon Trout River near Dodge City, MI

In order to demonstrate the differing temperature responses to moderate and high-intensity rainfall, we present the following case study. Discharge measurements come from USGS gage 04043244: East Branch Salmon Trout River near Dodge City, MI. The gage has a 10.2 square mile drainage area in a rural region of Michigan's Upper Peninsula. The corresponding precipitation gage is located at Big Bay 8 NW, MI. A map showing the locations of the two gages can be found in Figure 8.

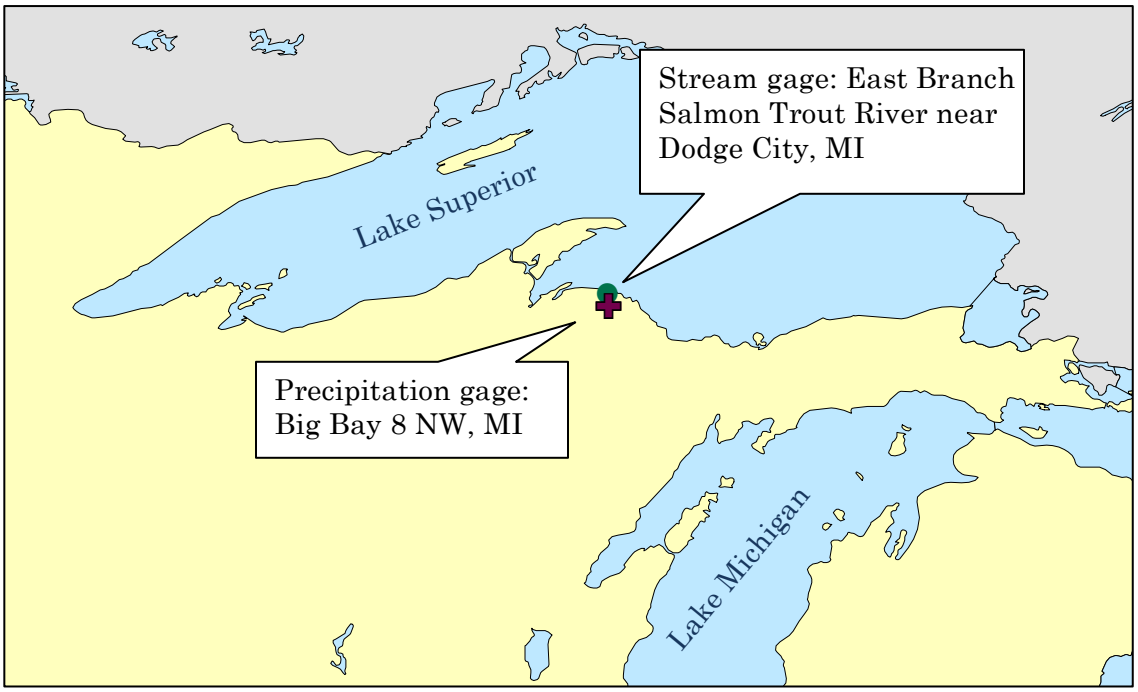

Figure 8: Location of the case study example showing the corresponding precipitation (green circle) and stream gages (maroon plus sign) on the Upper Peninsula of Michigan

3.1.1 Moderate-Intensity Rainfall

The example moderate-intensity rainfall event occurred on May 18, 2013. The maximum rainfall intensity was 0.1 in/15 min, or 0.4 in/hr. Discharge is shown by the blue

line and temperature by the red line, as seen in Figure 8a. The diurnal temperature variation can be seen in the peaks and troughs of the red line. During the peak in discharge caused by the rain event, the peak daytime temperature is less than the peaks on the neighboring two days.

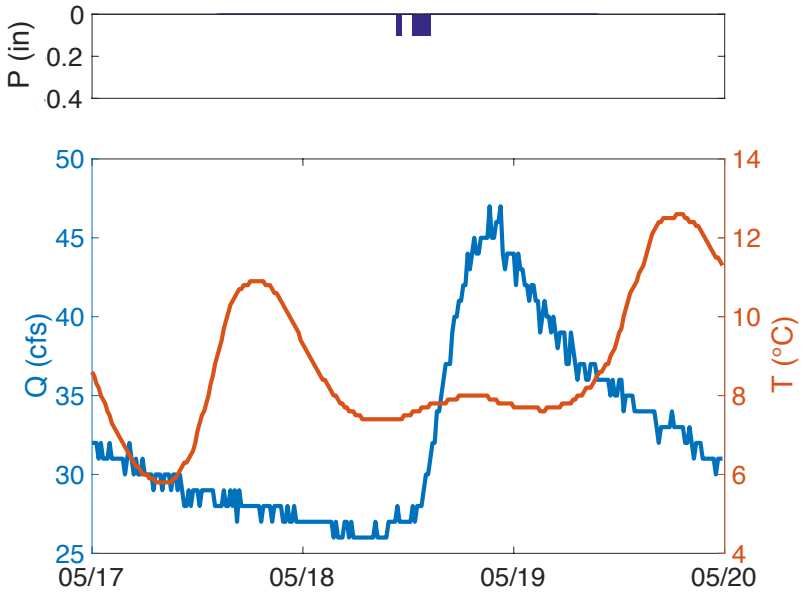

Figure 9: May 17-19, 2013: a moderate-intensity rainfall day with decreased daytime heating. Blue lines are discharge, red lines are temperature, and the above hyetograph shows rainfall amounts.

3.1.2 High-Intensity Rainfall

The example high-intensity event occurred June 21, 2012, as seen in Figure 9a. For this high intensity event, during which precipitation intensity peaked at 0.3 in/15 min (1.2 in/hr), the nighttime cooling was lessened in comparison to the temperature troughs of the neighboring two days.

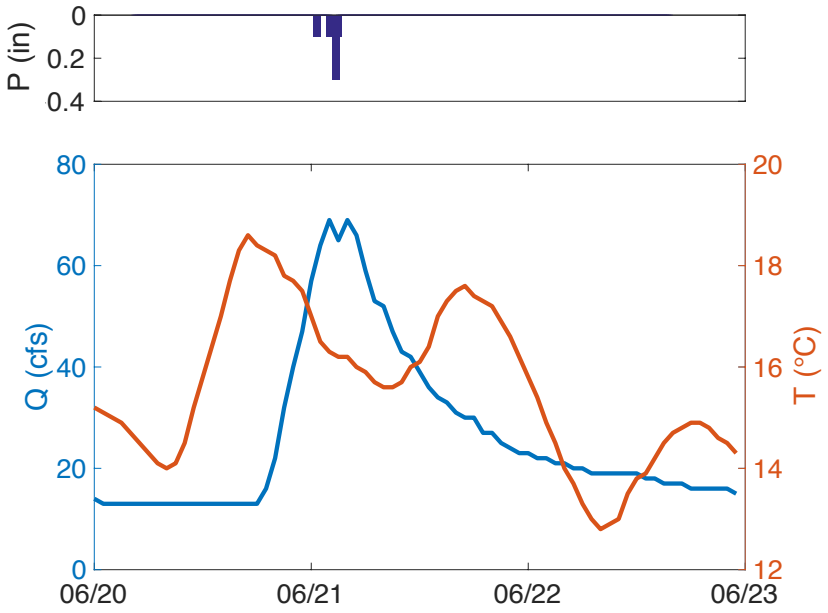

Figure 10: June 20-22, 2012: a high-intensity rainfall day with decreased nighttime cooling. Blue lines are discharge, red lines are temperature, and the above hyetograph shows rainfall amounts.

3.2 Gage Classification

The first analysis we completed was the evaluation of maximum daily hourly change in temperature, dT/dt. As previously described, through the comparison of daily maximum dT/dt, we were able to classify each individual gage as a SR system (higher dT/dt for high-intensity days) or a BR system (higher dT/dt for moderate-intensity days). To compare visually, mean daily maximum dT/dt for no, moderate-intensity, and high-intensity precipitation days were plotted separately as a deviation from the total mean for all days on record. The mean deviations for each precipitation classification can be seen in Figures 11a and 11b. 31 gages were classified as sensitive response (SR), 18 as buffered response (BR), 2 had a 95th high-intensity rainfall threshold equal to the minimum precision to which the rain gages could measure, and 1 gage had equal mean maximum dT/dt for moderate and

high-intensity gages. The latter 3 gages were unable to be classified as SR or BR through our techniques, so they were removed from further analysis.

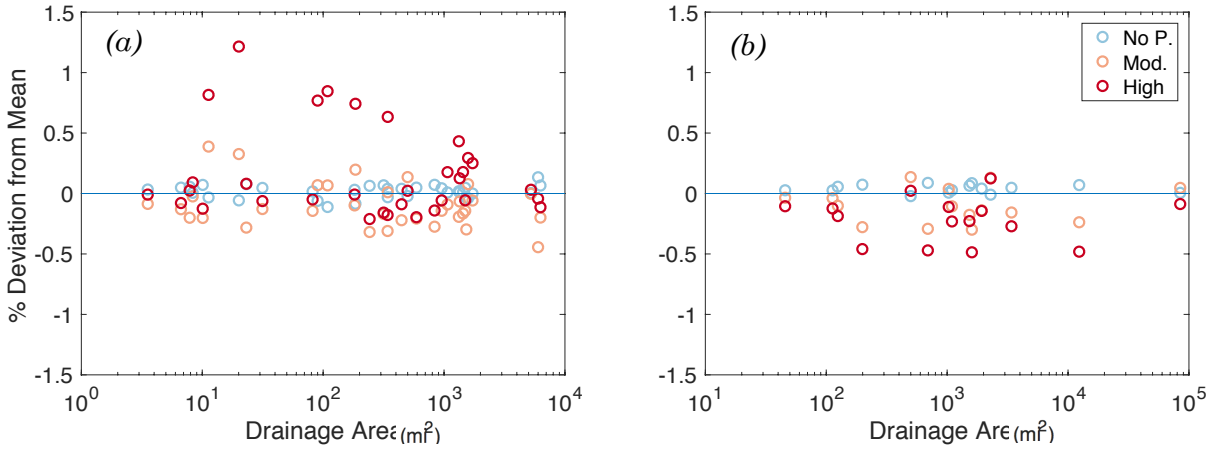

Figure 11: (a) SR systems: the deviation of mean daily maximum dT/dt for no (blue), moderate-intensity (orange), and high-intensity (red) precipitation days for rain-sensitive systems from the mean for all days. (b) BR systems: deviation of mean daily maximum dT/dt

Daily maximum dT/dt means for high-intensity precipitation days for SR gages fell on both sides of the total mean. Roughly half of the high-intensity SR means are above average, and half below. The gages with means above average have a stronger deviation than those below average. In Figure 9a, a noticeable trend is seen, as the deviation decreases with increasing drainage area. For SR systems, moderate-intensity days (SM) were a mix of above and below average daily maximum dT/dt. However, the deviation for SR moderate days was less than that of SR high-intensity days. For BR systems, both moderate and high-intensity means are mostly below average (Figure 9b). For both sensitive and buffered response systems, no-precipitation days were around average.

3.3 Discharge

3.3.1 Maximum Q

The next parameter examined was the daily maximum discharge (Q), as seen in Figures 12a and 12b. For SR systems, high-intensity days were generally far above the average. Moderate-intensity days in SR systems were also above average, but not to the positive extent of deviation seen observed for high-intensity days. For BR systems, the means of high-intensity and moderate-intensity days were both above average, but the deviation from the mean for high-intensity days was less extreme than their SR counterparts.

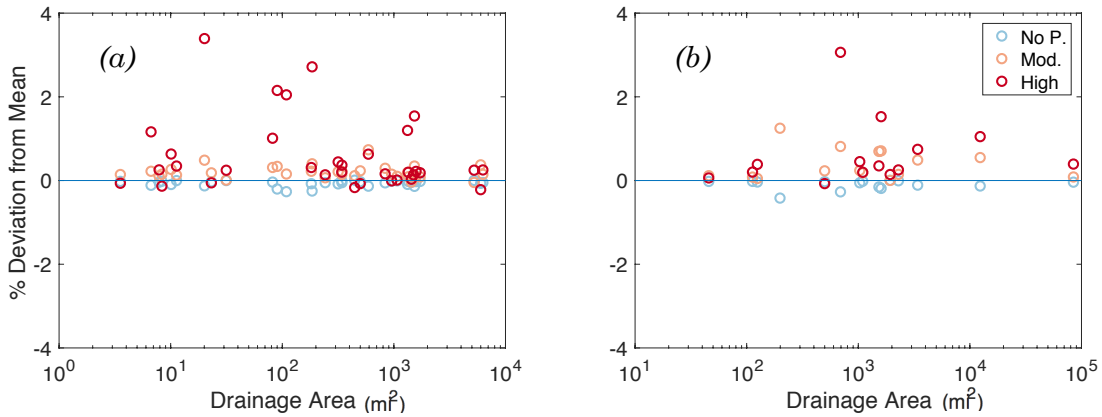

Figure 12: (a) SR systems: the deviation of mean daily maximum Q for no (blue), moderate-intensity (orange), and high-intensity (red) precipitation days for rain-sensitive systems from the mean for all days. (b) BR systems: deviation of mean daily maximum Q

3.3.2 Maximum dQ/dt

Patterns of deviation from the mean daily maximum hourly dQ/dt were similar for SR and BR systems and can be seen in Figures 13a and 13b. In both types of systems, both moderate-intensity and high-intensity days were above average, with high-intensity days having the greatest positive deviation.

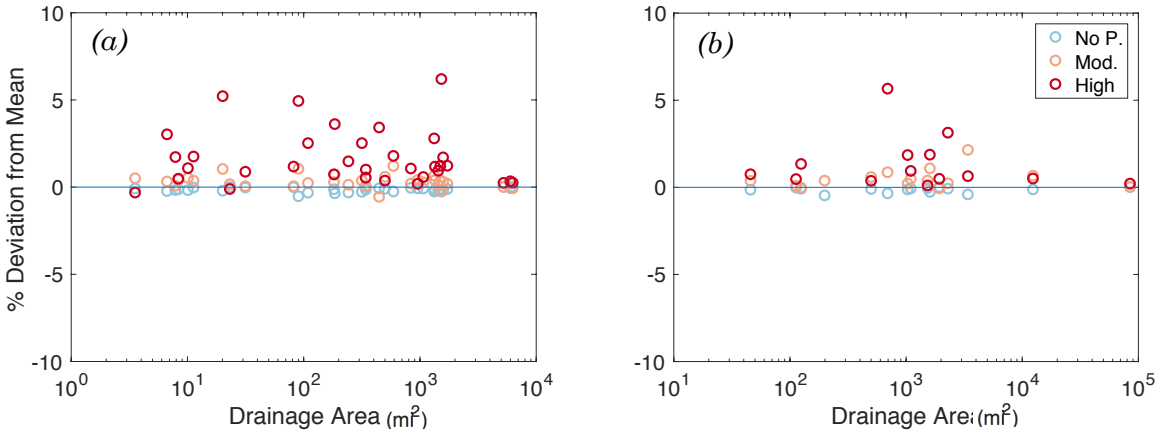

Figure 13: (a) SR systems: the deviation of mean daily maximum dQ/dt for no (blue), moderate-intensity (orange), and high-intensity (red) precipitation days for rain-sensitive systems from the mean for all days. (b) BR systems: deviation of mean daily maximum dQ/dt

3.3.3 Q Range

Similarly, as seen in Figures 14a and 14b, both SR and BR systems had above average mean *Q* range for both moderate-intensity and high-intensity rainfall days. High-intensity days had a relatively higher mean deviation for both SR and BR gages.

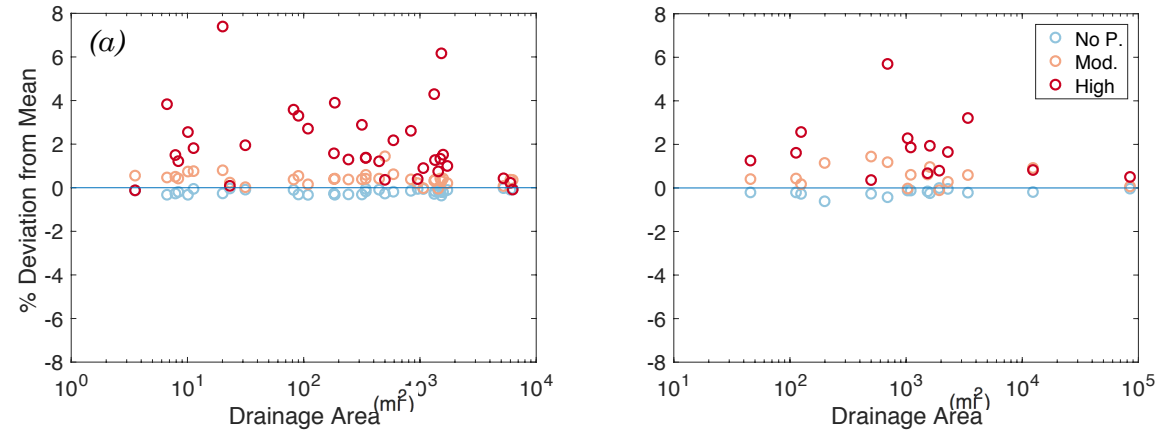

Figure 14: (a) SR systems: the deviation of mean daily Q range for no (blue), moderate-intensity (orange), and high-intensity (red) precipitation days for rain-sensitive systems from the mean for all days. (b) BR systems: deviation of mean daily Q range

3.4 Temperature

3.4.1 Maximum T

For mean daily maximum *T*, SR gages show a division between moderate and high-intensity days, as seen in Figure 15a. High-intensity days generally had above average mean daily maximum *T*, while moderate days were generally below average. For BR gages, shown in Figure 15b moderate days were similarly below average, but the deviation of high-intensity days was mixed. For roughly half of the buffered gages, high-intensity days had above average mean daily maximum *T*. However, the other half of gages had high-intensity means below average.

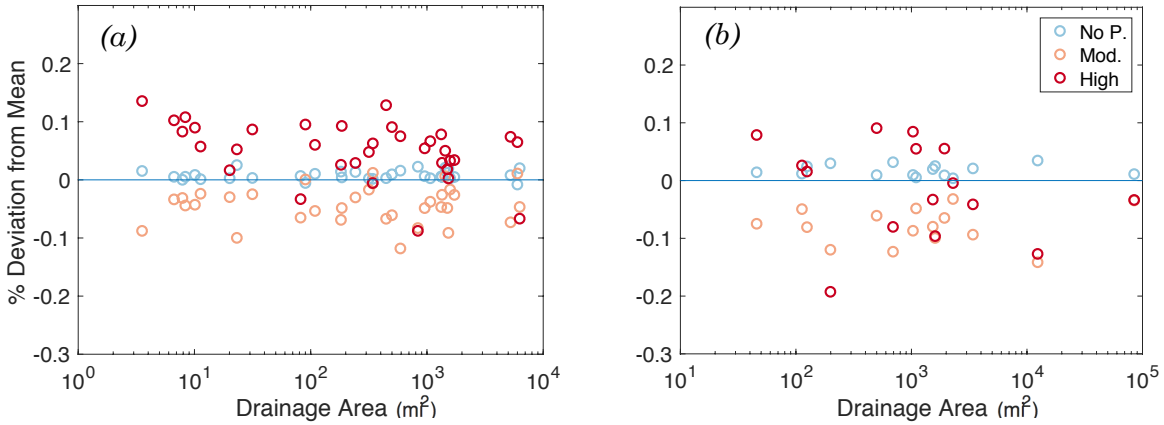

Figure 15: (a) SR systems: the deviation of mean daily maximum T for no (blue), moderate-intensity (orange), and high-intensity (red) precipitation days for rain-sensitive systems from the mean for all days. (b) BR systems: deviation of mean daily maximum T

3.4.2 T Range

The mean temperature range, as seen in Figures 16a and 16b, was mostly below average for moderate and high-intensity rainfall days for both SR and BR systems. However, SR systems did have several gages with above average mean daily *T* range.

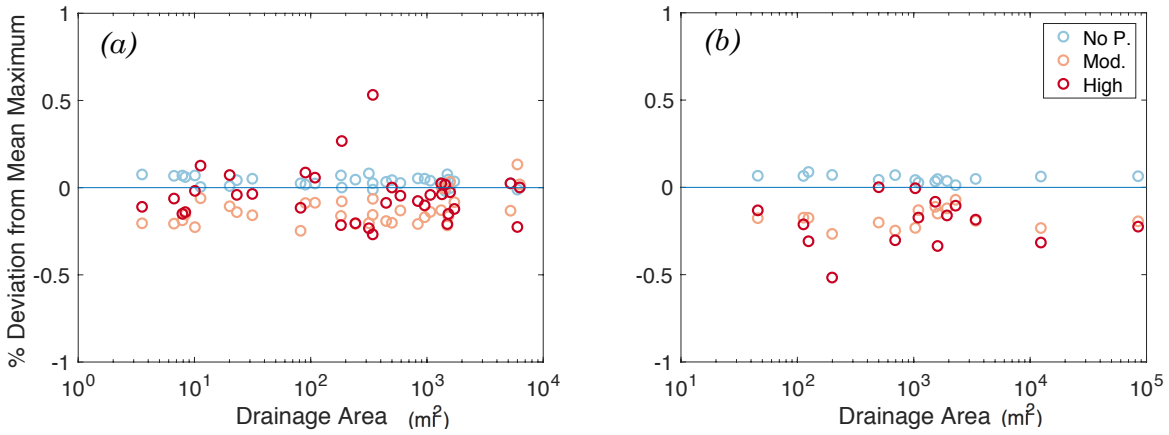

Figure 16: (a) SR systems: the deviation of mean daily T range for no (blue), moderate-intensity (orange), and high-intensity (red) precipitation days for rain-sensitive systems from the mean for all days. (b) BR systems: deviation of mean daily T range

3.4.3 Heat Accumulation

The mean daily heat accumulation was below average for moderate-intensity days for both SR and BR gages, as seen in Figures 17a and 17b. For high-intensity days, SR gages showed a mostly above average heat accumulation. BR gages, on the other hand, showed a mixed response. While several gages had above average mean daily accumulated heat, the positive deviation was not as large as their SR counterparts. Roughly half of the BR gages showed below average heat accumulation for high-intensity precipitation days.

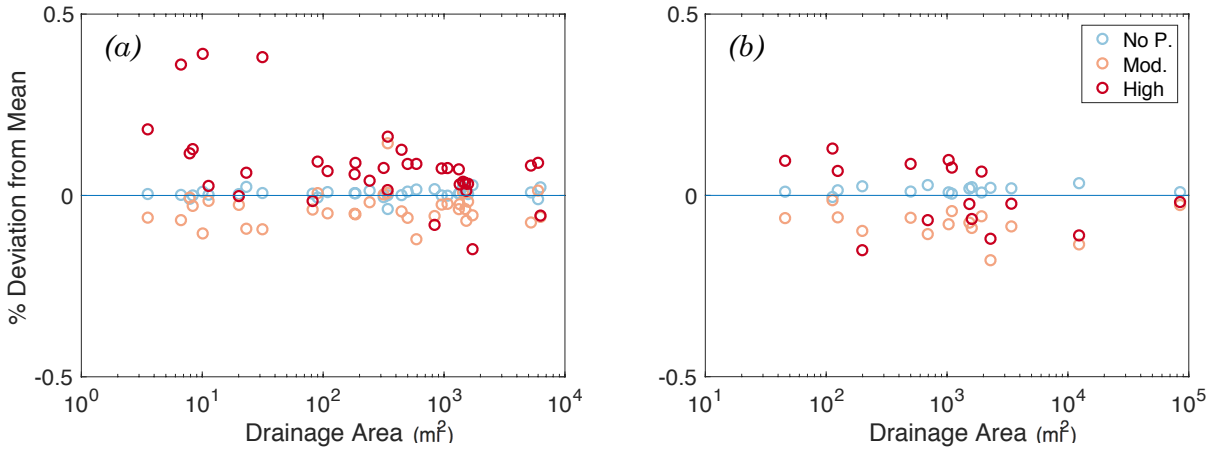

Figure 17: (a) SR systems: the deviation of mean daily heat accumulation for no (blue), moderate-intensity (orange), and high-intensity (red) precipitation days for rain-sensitive systems from the mean for all days. (b) BR systems: deviation of mean heat accumulation

3.5 Drainage Area Conditions

3.5.1 Impervious Surface Area

Percent impervious surface area for the study area ranged from 0.06% in the rural immediate drainage area of the Bad River near Odanah, WI to around 47% in the urban drainage area surrounding the River Rouge gage at Detroit, MI. All of the drainage areas in the BR category had impervious surface areas below 10%, as seen in Figure 18b. All of the drainage areas with impervious surface area over 10% had been previously classified based on daily maximum dT/dt as SR gages, as seen in Figure 18a. While 6 of the 34 SR gages had impervious surface area over 10%, with 4 of the 6 over 30% impervious, the remaining 28 SR gages had low impervious surface areas comparable to percentages found for BR gages.

(a) *(b)*

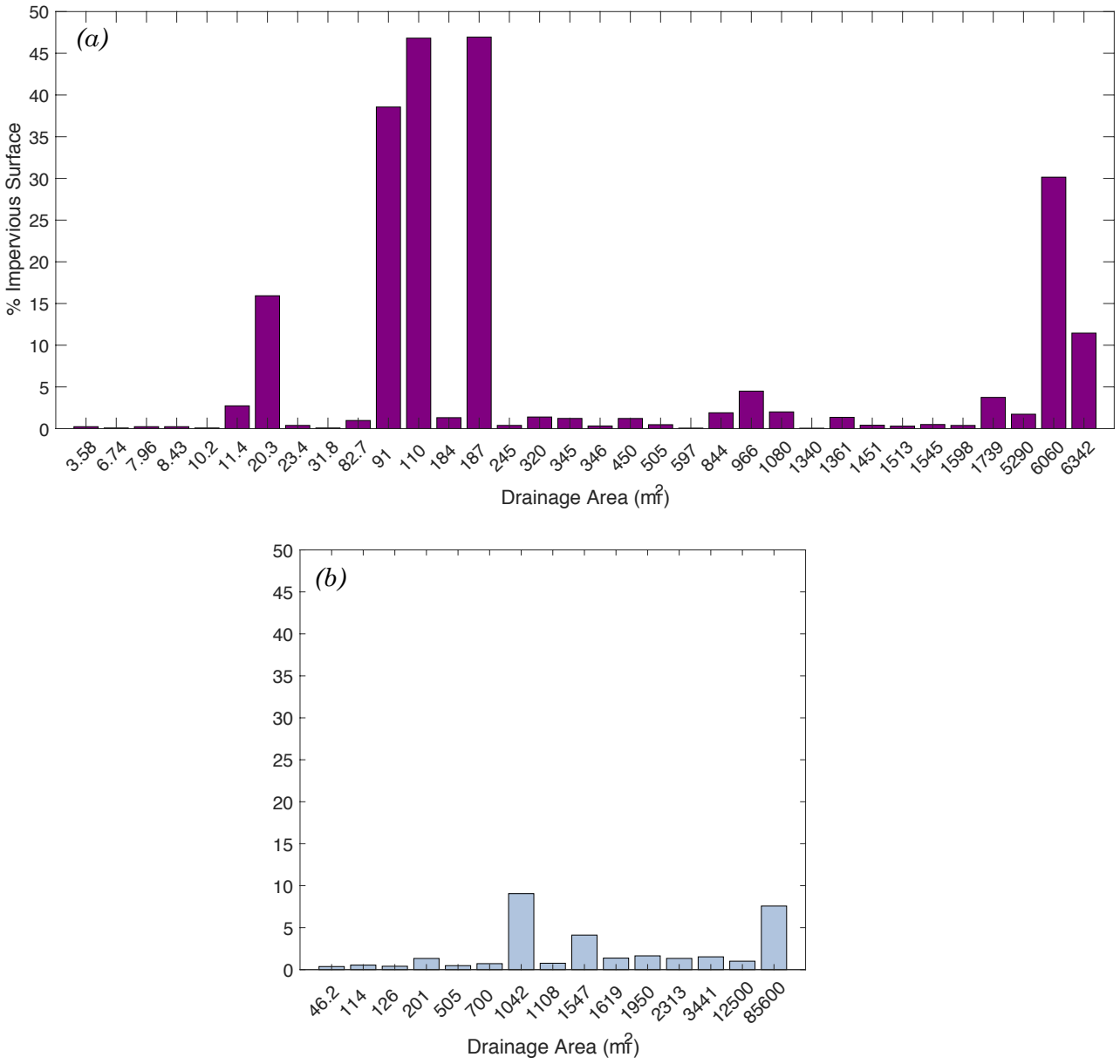

Figure 18: (a) Percent impervious surface area for the SR systems (purple) and (b) BR systems (gray). Areas are show with respect to increasing drainage area.

3.5.2 Hydrologic Soil Group

The mean percentage of type D hydrologic soil group was calculated separately for SR and BR gages for both undrained soil and drained soil conditions. Type D soil has the lowest infiltration rate and the highest proclivity for runoff. SR gages had a higher mean

percentage of type D soils for both undrained and drained soil conditions, as seen in Figure 19. However, a two-sample t-test revealed that the difference was statistically significant for neither undrained nor drained conditions.

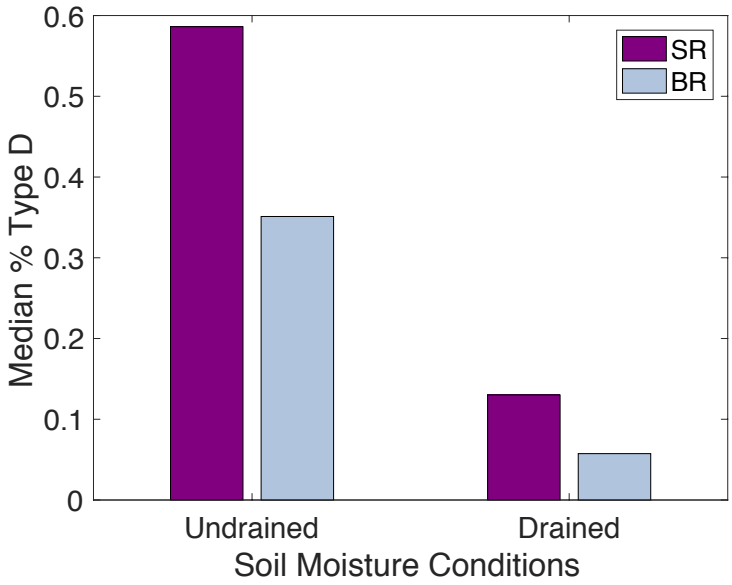

Figure 19: Median percentage of the HUC 12 drainage area with type D soil for sensitive response (purple) and buffered response systems (gray) for both drained and undrained soil conditions.

3.5.3 Antecedent Moisture

Antecedent moisture was measured for each day as the total rainfall of the previous five days, as described by the National Engineering Handbook (NRCS, 1993). Antecedent moisture was compared to daily maximum hourly change in temperature (dT/dt) as seen in Figures 20a, 20b, 21a, and 21b.

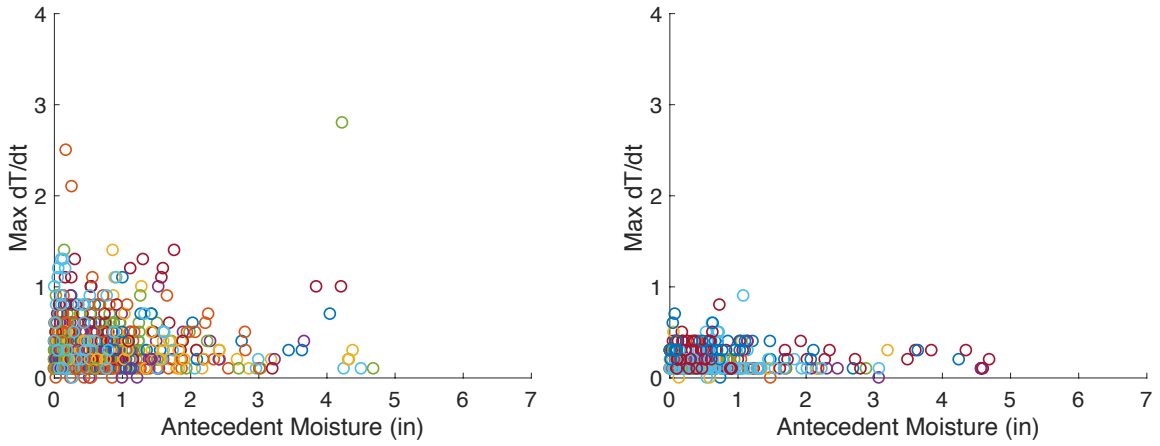

(a) *(b)*

Figure 20: High-intensity rainfall days' antecedent moisture against daily maximum dT/dt for (a) SR gages and (b) BR gages. Each point represents a single 24-hour period

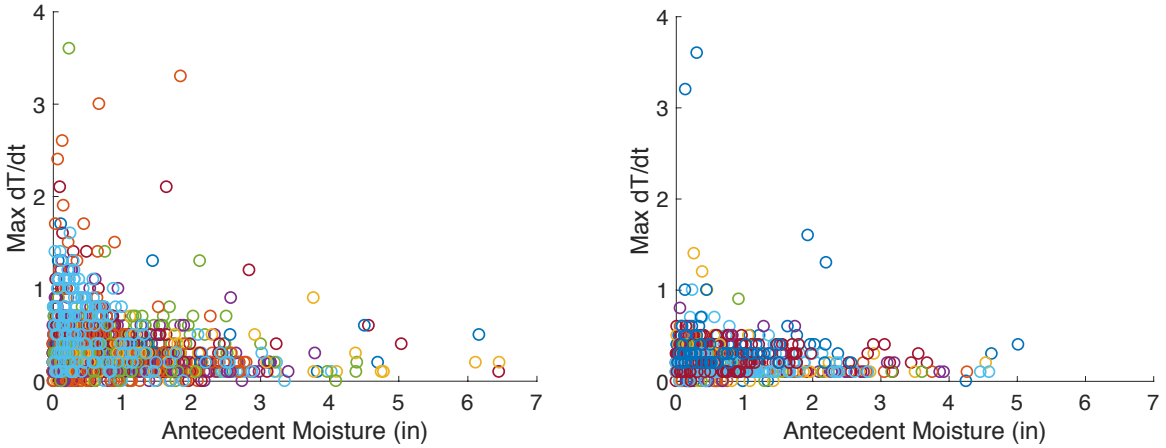

(a) *(b)*

Figure 21: Moderate-intensity rainfall days' antecedent moisture against daily maximum dT/dt for (a) SR gages and (b) BR gages. Each point represents a single 24-hour period.

Separated by gage type classification and rainfall intensity, and fit with a linear regression model, the four different categories achieved the following results seen in Table 6:

Table 6: Antecedent Moisture Linear Regression

Rainfall Intensity	System Type	Estimated coefficient (slope)	p-value
High	SR	0.035	0.049
High	BR	-0.014	0.082
Moderate	SR	0.035	0.049
Moderate	BR	-0.014	0.082

Based on the p-value and using 0.05 as a threshold for statistical significance, sensitive response systems had a significant, though not extreme, positive trend in increasing daily maximum dT/dt with increasing antecedent moisture. BR systems did not have a statistically significant trend for either high-intensity or moderate-intensity days.

3.6 Application to Midwestern Trout Species

The range of daily maximum temperature values for each gage were examined with respect to the top end of the preferred temperature range for the Rainbow Trout and Brook Trout, 14°C for both species. The daily maximum temperatures were represented by boxplots and separated by system type. In comparison to no rainfall days (Figures 22a and 22b) and moderate-intensity days (Figures 23a and 23b), the range of high-intensity rainfall days (Figures 24a and 24b) did not extend as frequently into the preferred temperature range. 31 of the 52 gages did not reach low enough temperatures to be in the preferred temperature range, represented by the horizontal reference line at 14°C.

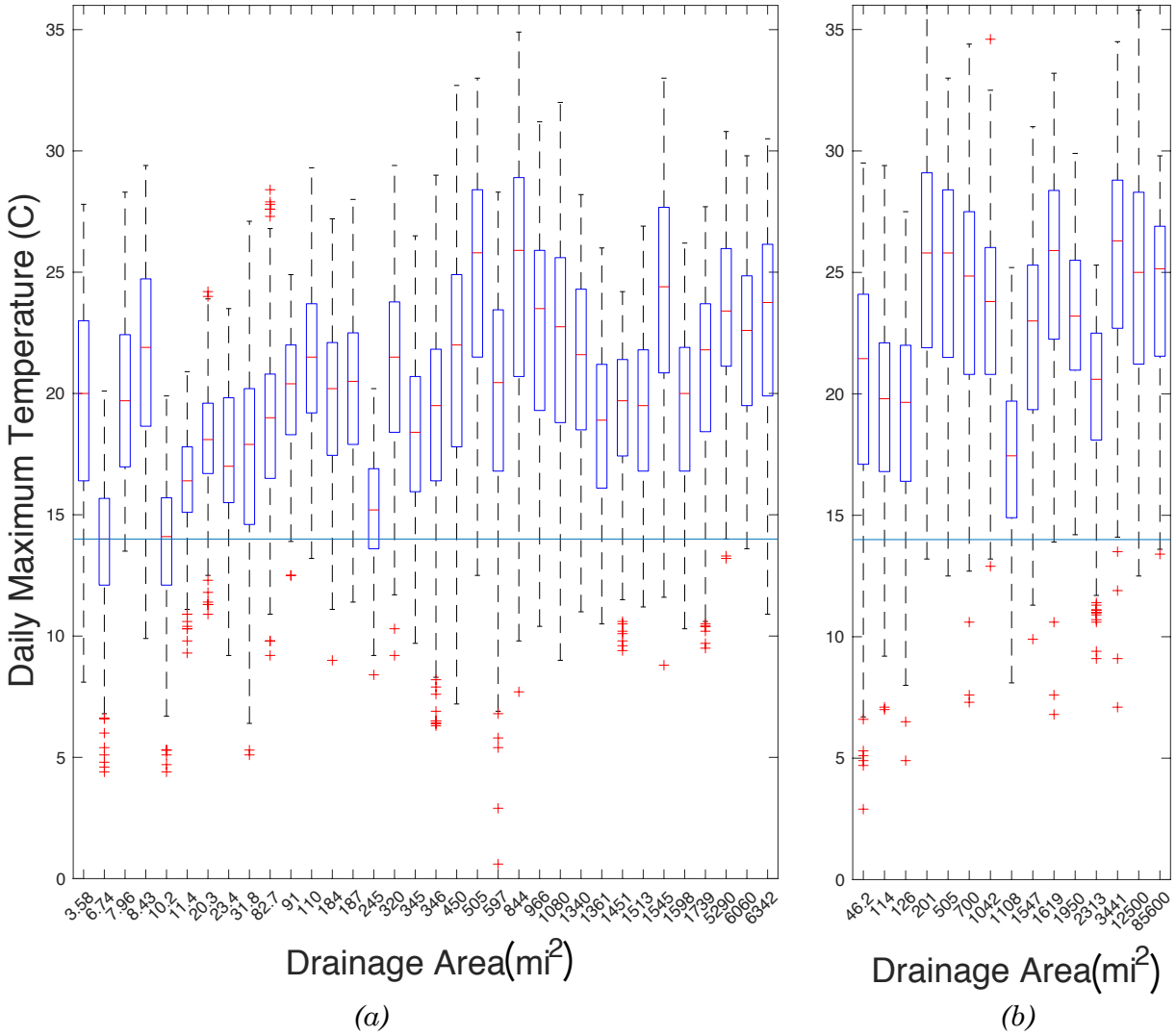

Figure 22: Boxplots of daily maximum temperature for no-rainfall days for individual gages, marked by their respective drainage area. The upper limit of the preferred temperature range of the brook and rainbow trout is marked by the horizontal line at 14°C. (a) Sensitive response systems. (b) Buffered response systems.

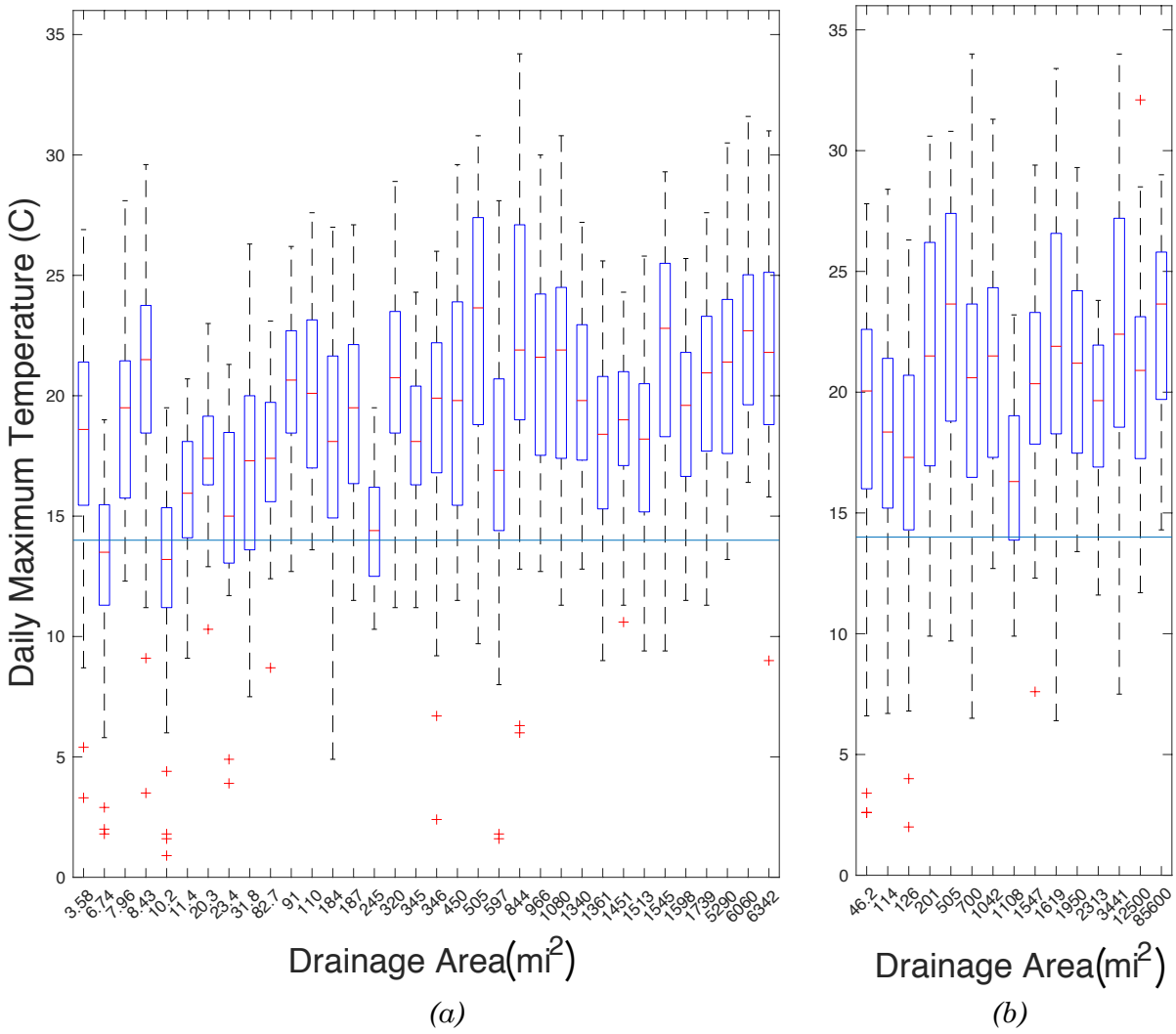

Figure 23: Boxplots of daily maximum temperature for moderate-intensity rainfall days for individual gages, marked by their respective drainage area. The upper limit of the preferred temperature range of the brook and rainbow trout is marked by the horizontal line at 14°C. (a) Sensitive response systems. (b) Buffered response systems.

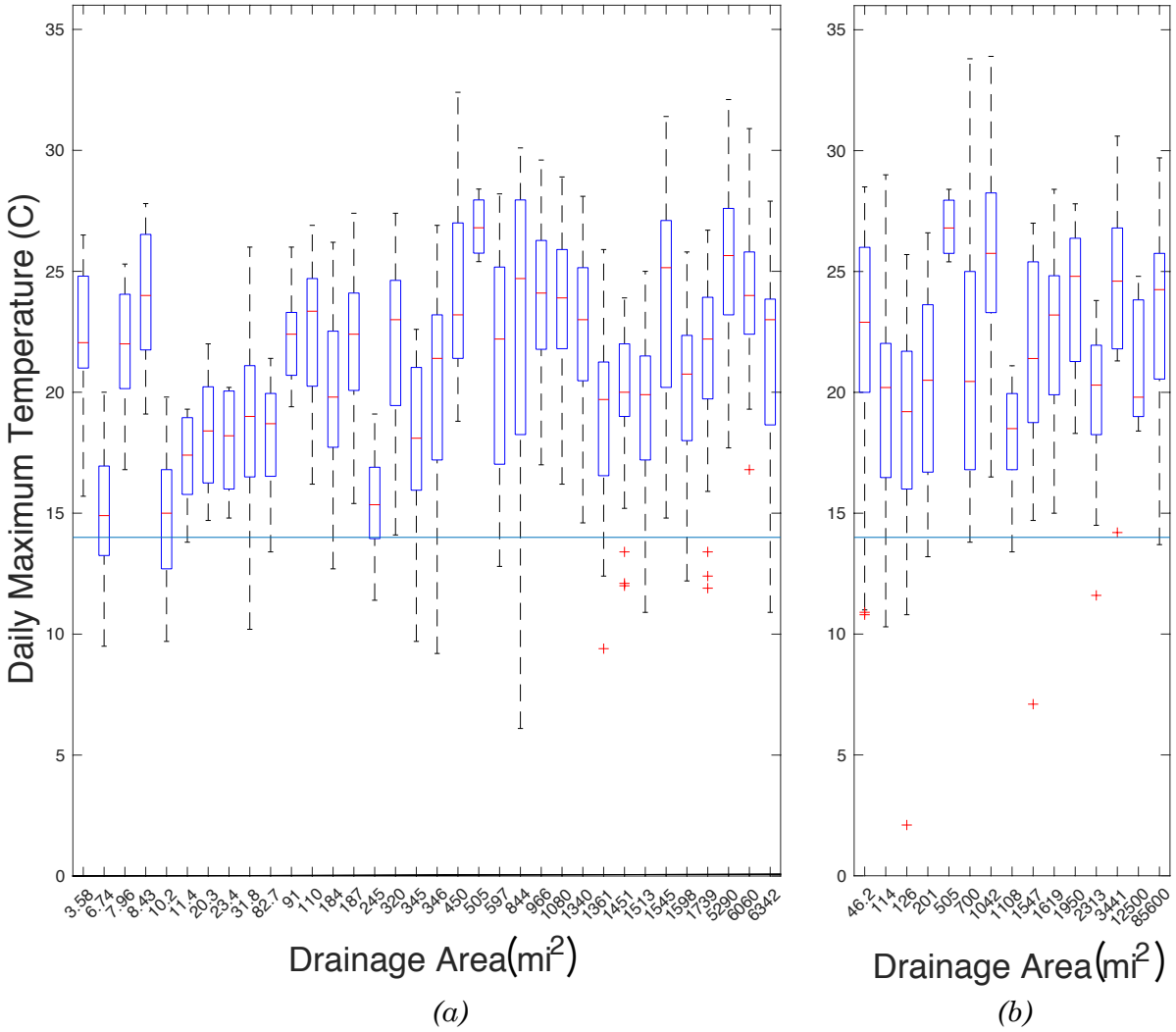

Figure 24: Boxplots of daily maximum temperature for high-intensity rainfall days for individual gages, marked by their respective drainage area. The upper limit of the preferred temperature range of the brook and rainbow trout is marked by the horizontal line at 14°C. (a) Sensitive response systems. (b) Buffered response systems.

4. Discussion

In this study, we divided the gages into two different classifications based on their thermal temperature responses to high-intensity rainfall. We can surmise, based on the higher impervious surface areas and soil type D percentages that the reason that some gages have a greater mean maximum daily dT/dt for high-intensity rainfall (SR gages) is because these are shallow subsurface flow dominated systems. The buffered response (BR) gages could be then presumed to be groundwater flow dominated. However, a main limitation of this study is related to the unavailability of data. The distinction of shallow subsurface flow versus groundwater flow-dominated systems could be more clearly defined with the accessibility of shallow subsurface and groundwater flow data. Additionally, data related to groundwater temperature and soil moisture were not available. This lack of data forced several assumptions in the study including the approximation that groundwater temperature is equal to mean annual surface air temperature and that soil moisture is equal to the total of the previous five days' rainfall. Ideally, stream gages and precipitation gages would be collocated. As this was not the case, the Thiessen polygon method was utilized to assign the nearest precipitation gage to each stream gage.

Impervious surface area, soil type, and antecedent moisture conditions were examined in an attempt to explain the difference in responses seen between SR and BR gages. All of the gages with impervious surface area above 10% were classified as SR gages. Impervious surfaces, by definition, allow for less infiltration and would, as expected, have increased runoff and stream temperatures with high-intensity rain events. Soil type was not shown to be statistically significant in this study, though SR gages showed, on average, higher percentages of soils with reduced infiltration rates. Only the immediate HUC 12 surrounding each stream gage was used for analysis of impervious surface area

and soil type, so an extension of the evaluation of soil type to include the entire drainage area might yield different results. Antecedent moisture also did not have provide a noteworthy explanation for the difference in temperature responses.

The scope of this study utilized data from many gages and many dates, which meant that the only reasonable way to process the data was through statistics, such as means and quantiles. In order to fully understand why different storms trigger different temperature responses, future work might focus on precipitation and stream temperature at an event-by-event level.

The main motivations for this study revolve around temperature dependent ecosystem health and power plant generation. Laws require that thermal pollution be regulated in order to protect the flora and fauna that are dependent on water temperature. As mentioned earlier, some species of fish have been observed to move to colder regions of the water body when their current location becomes uncomfortable. However, if temperatures warm with high-precipitation intensity, as has been observed in this thesis, these thermal refugia may decrease in availability. Additionally, if temperatures warm, power plants will have to decrease production to oblige with thermal regulations. This is additionally problematic that warmer temperatures decrease production because power demands are highest in the summer. However, there does exist a limit to which water temperature can warm. If we assume that the primary source of heat in a stream is from solar radiation, and we ignore the effects of anthropogenic sources such as thermoelectric power plant effluent, then the stream temperature cannot rise higher than air temperature.

Our analysis of dT/dt and division of gages into SR and BR, raises an important distinction: while warming stream temperatures were observed in response to high-intensity rainfall for some gages, they were not observed for all. Fish in BR systems, for example, may not be affected by a change related to high-intensity rainfall. Similarly,

thermoelectric power plants may not need to reduce production for temperature spikes related to high-intensity rainfall.

Alternatively, additional research would be necessary to understand the response of aquatic life and power plants that are affected. Fish could possibly have adaptation strategies to cope with hot flashes and mean rising temperatures. Additionally, technology used in power generation could improve as to adopt more efficient cooling methods. Now that the binary question: *Does high-intensity rainfall cause an increase in temperature?* has been addressed, further analysis should explore the characteristics of temperature increase. Understanding the features of high-intensity rainfall related temperature changes, for example, the duration of elevated temperature levels, will be helpful in understanding the response that fish and power plant operators need to take.

5. Conclusion

This thesis explored the effect of rainfall intensity on stream temperature during summer months in the Upper Midwestern United States through 52 USGS gages in Iowa, Wisconsin, and Michigan. The findings revealed that for majority of gages, mean daily maximum temperature and total daily accumulated heat was higher for high-intensity precipitation days when compared to moderate-intensity days.

The data was divided into two categories based on whether the mean daily maximum hourly change in temperature (dT/dt) was greater for high-intensity days (SR systems) or moderate-intensity days (BR systems). We attempted to explain the difference in dT/dt responses through impervious surface area, soil type, and the antecedent soil moisture for individual events. While all of the highly impervious gages were classified as SR gages, not all gages in the SR category were highly impervious. Gages in the SR category had, on average, higher percentages of type D soil, which has the lowest infiltration rate and the highest proclivity for runoff. Antecedent moisture showed a slight trend suggesting an increase in dT/dt for higher antecedent moisture for SR gages.

Future work might examine stream temperature response on a smaller event scale in order to further unlock the mechanics of temperature response to extreme precipitation intensity. Understanding temperature response is vital to prepare for the effect of high-intensity precipitation in the context of riverine-dependent industries such as fisheries and thermoelectric power generation.

Bibliography

Allen, T., Southwick, R., 2008. Sportfishing in America. Alexandria, VA.

Angel, J.R., Huff, F.A., 1997. Changes in Heavy Rainfall in Midwestern United States. J. Water Resour. Plan. Manag. 123, 246–249.

Becker, C.D., Wolford, M.G., 1980. Thermal Resistance of Juvenile Salmonids Sublethally Exposed to Nickel, Determined by the Critical Thermal Maximum Method. Environ. Pollut. 21, 181–189.

Beitinger, T.L., Bennett, W.A., Mccauley, R.W., 2000. Temperature tolerances of North American freshwater fishes exposed to dynamic changes in temperature. Environ. Biol. Fishes 58, 237–275.

Blakey, J.F., 1966. Temperature of Surface Waters in the Conterminous United States.

Caissie, D., 2006. The thermal regime of rivers: A review. Freshw. Biol. doi:10.1111/j.1365-2427.2006.01597.x

Constantz, J., 1998. Interaction between stream temperature, streamflow, and groundwater exchanges in alpine streams. Water Resour. Res. 34, 1609–1615. doi:10.1029/98WR00998

Currie, R.J., Bennett, W.A., Beitinger, T.L., 1998. Critical thermal minima and maxima of three freshwater game-fish species acclimated to constant temperatures. Environ. Biol. Fishes 51, 187–200.

Dehring, T., Krueger, C.C., 2008. Brook Trout. Madison, WI.

Dehring, T., Krueger, C.C., Hansen, M.J., 2008. Rainbow Trout. Madison, WI.

Eaton, J.G., Scheller, R.M., 1996. Effects of climate warming on fish thermal habitat in streams of the United States. Limnol. Ocean. 41, 1009–1115.

Evans, E.C., Mcgregor, G.R., Petts, G.E., 1998. River energy budgets with special reference to river bed processes. Hydrol. Process. 12, 575–595.

Ficklin, D.L., Luo, Y., Stewart, I.T., Maurer, E.P., 2012. Development and application of a hydroclimatological stream temperature model within the Soil and Water Assessment Tool 48, 1–16. doi:10.1029/2011WR011256

Fiedler, F.R., 2003. Simple , Practical Method for Determining Station Weights Using Thiessen Polygons and Isohyetal Maps. J. Hydrol. Eng. 8, 219–221.

Fischer, E.M., Knutti, R., 2015. Anthropogenic contribution to global occurrence of heavy-precipitation and high-temperature extremes. Nature 5. doi:10.1038/NCLIMATE2617

Groisman, P.Y., Knight, R.W., Easterling, D.R., Karl, T.R., Hegerl, G.C., Razuvaev, V.N., 2005. Trends in intense precipitation in the climate record. J. Clim. 18, 1326–1350. doi:10.1175/JCLI3339.1

Karl, T.R., Knight, R.W., 1998. Secular Trends of Precipitation Amount, Frequency, and Intensity in the United States. Bull. Am. Meteorol. Soc. 231–241. doi:10.1175/1520-0477(1998)079<0231:STOPAF>2.0.CO;2

Kelleher, C., Wagener, T., Gooseff, M., Mcglynn, B., Mcguire, K., Marshall, L., 2012. Investigating controls on the thermal sensitivity of Pennsylvania streams 5. doi:10.1002/hyp.8186

Koch, H., Vögele, S., 2009. Dynamic modelling of water demand, water availability and adaptation strategies for power plants to global change. Ecol. Econ. 68, 2013–2039. doi:10.1016/j.ecolecon.2009.02.015

Lee, R.M., Rinne, J.N., 1980. Critical Thermal Maxima of Five Trout Species in the Southwestern United States. Trans. Am. Fish. Soc. 109.

Kottek, M., Grieser, J., Beck, C., Rudolf, B., Rubel, F., 2006. World Map of the Köppen-Geiger climate classification updated. Meteorol. Zeitschrift 15, 259–263. doi:10.1127/0941-2948/2006/0130

MacDonald, R.J., Boon, S., Byrne, J.M., Silins, U., 2014. A comparison of surface and subsurface controls on summer temperature in a headwater stream. Hydrol. Process. 28, 2338–2347. doi:10.1002/hyp.9756

Maheu, A., Poff, N.L., St-Hilaire, A., 2016. A Classification of Stream Water Temperature Regimes in the Conterminous USA. River Res. Appl. 32, 896–906. doi:10.1002/rra.2906

Mays, L.W., 2011. Water Resources Engineering, 2nd ed. John Wiley & Sons, Hoboken, NJ.

McCuen, R., 2004. Hydrologic Analysis and Design, 3rd ed. Pearson Education, New York, NY.

Mosley, P.M., McKerchar, A.I., 1993. Streamflow, in: Handbook of Hydrology. McGraw-Hill, Inc., p. 81.

Milly, P.C.D., Betancourt, J., Falkenmark, M., Hirsch, R.M., Kundzewicz, Z.W., Lettenmaier, D.P., Stouffer, R.J., 2008. Stationarity Is Dead: Whither Water Management? Science (80-.). 319, 573–574.

Moore, R.D., Leach, J.A., Knudson, J.M., 2014. Geometric calculation of view factors for stream surface radiation modelling in the presence of riparian forest. Hydrol. Process. 28, 2975–2986. doi:10.1002/hyp.9848

NRCS, 1993. Storm Rainfall Depth, in: National Engineering Handbook.

Nelson, K.C., Palmer, M.A., 2007. Stream Temperature Surges Under Urbanization. J. Am 43, 440–452.

Sevacherian, V., Stern, V.M., Mueller, A.J., 1977. Heat Accumulation for Timing Lygus (Hemiptera-(Heteroptera)-Miridae) Control Measures in a Safflower-Cotton Complex. J. Econ. Entomol. 70, 399–402.

Sinokrot, B.A., Stefan, H.G., 1994. Stream Temperature Sensitivity to Weather and Bed Parameters. J. Hydraul. Eng. 120, 722–736.

Somers, K.A., Bernhardt, E.S., Mcglynn, B.L., Urban, D.L., 2016. Downstream Dissipation of Storm Flow Heat Pulses: A Case Study and its Landscape-Level Implications 1. J. Am. Water Resour. Assoc. 52. doi:10.1111/1752-1688.12382

Sun, X., Lall, U., Palmer, M.A., Moore, R.D., Leach, J.A., Knudson, J.M., Macdonald, R.J., Boon, S., Byrne, J.M., Silins, U., Fischer, E.M., Knutti, R., Fiedler, F.R., Currie, R.J., Bennett, W.A., Beitinger, T.L., Centre, P.C., Wetterdienst, D., Blakey, J.F., Beitinger, T.L., Bennett, W.A., Mccauley, R.W., 2014. Critical thermal minima and maxima of three freshwater game-fish species acclimated to constant temperatures 15, 187–200. doi:10.1127/0941-2948/2006/0130

Teegavarapu, R.S. V, Chandramouli, V., 2005. Improved weighting methods, deterministic and stochastic data-driven models for estimation of missing precipitation records. J. Hydrol. 312, 191–206. doi:10.1016/j.jhydrol.2005.02.015

Thiessen, A.H., 1911. Precipitation Averages for Large Areas. Mon. Weather Rev. 1082–1084.

Torgersen, C.E., Price, D.M., Li, H.W., Mcintosh, B.A., 1999. Multiscale Thermal Refugia and Stream Habitat Associations of Chinook Salmon in Northeastern Oregon. Ecol. Appl. 9, 301–319.

Van Vliet, M.T.H., Sheffield, J., Wiberg, D., Wood, E.F., 2016. Impacts of recent drought and warm years on water resources and electricity supply worldwide. Environ. Res. Lett. 11.

Van Vliet, M.T.H., Yearsley, J.R., Ludwig, F., Vögele, S., Lettenmaier, D.P., Kabat, P., 2012. Vulnerability of US and European electricity supply to climate change. Nat. Clim. Chang. 2, 676–681. doi:10.1038/nclimate1546

Villarini, G., Smith, J.A., Baeck, M.L., Vitolo, R., Stephenson, D.B., Krajewski, W.F., 2011. On the frequency of heavy rainfall for the Midwest of the United States. J. Hydrol. 400, 103–120. doi:10.1016/j.jhydrol.2011.01.027

Villarini, G., Smith, J.A., Vecchi, G.A., 2013. Changing frequency of heavy rainfall over the central United States. J. Clim. doi:10.1175/JCLI-D-12-00043.1

Appendix

A1. Featured Gage Sites by Drainage Area

D.A. (mi^2)	Stream Gage	USGS Gage No.	Precipitation Gage	Rain Sens.
3.58	North Creek at Trout Lake near Boulder Junction, WI	05357230	Rainbow Reservoir Lake Tomahawk, WI US	S
6.74	Salmon Trout River near Big Bay, MI	04043238	Big Bay 8 NW, MI US	S
7.96	Stevenson Creek @ Ct Hwy M Nr Boulder Junction, WI	05357225	Rainbow Reservoir Lake Tomahawk, WI US	S
8.43	Allequash Creek @ Ct Hwy M Nr Boulder Junction, WI	05357215	Rainbow Reservoir Lake Tomahawk, WI US	S
10.2	East Branch Salmon Trout River near Dodge City, MI	04043244	Big Bay 8 NW, MI US	S
11.4	Black Earth Creek nr Brewery Rd at Cross Plains, WI	05406457	Charmany Farm, WI US	S
20.3	Badger Mill Creek at Verona, WI	05435943	Charmany Farm, WI US	S
23.4	Trout Creek at Tenth Street Near Bloomer, WI	53674967	Chippewa Falls, WI US	S
31.8	Yellow Dog River near Big Bay, MI	04043275	Big Bay 8 NW, MI US	S
46.2	Trout River At Trout Lake near Boulder Junction, WI	05357245	Rainbow Reservoir Lake Tomahawk, WI US	I
82.7	Sugar River near Verona, Wi	05435950	Charmany Farm, WI US	S
91	Lower River Rouge at Dearborn, MI	04168400	Ypsilanti E Michigan University, MI US	S
110	Middle River Rouge at Dearborn Heights, MI	04167150	Ypsilanti E Michigan University, MI US	S

114	Red River at Morgan Road Near Morgan, WI	04077630	White Lake 1 S, WI US	I
126	Namekagon River at Leonards, WI	05331833	Hayward Ranger Station, WI US	I
184	Prairie River near Merrill, WI	05394500	Merrill, WI US	S
187	River Rouge at Detroit, MI	04166500	Ypsilanti E Michigan University, MI US	S
201	Old Mans Creek near Iowa City, IA	05455100	Iowa City, IA US	I
245	Pine River at High School Bridge Nr Hoxeyville, MI	04125460	Scottville 2 SE, MI US	S
320	Rifle River near Sterling, MI	04142000	Gladwin, MI US	S
345	Little Muskegon River near Oak Grove, MI	04121944	Kent City 2 S, MI US	S
346	Sturgeon River near Alston, MI	04041500	Alberta Ford For Cen, MI US	S
450	Ford River near Hyde, MI	04059500	Escanaba, MI US	S
505	North Fork Maquoketa River near Fulton, IA	05418400	Cascade, IA US	I
597	Bad River near Odanah, WI	04027000	Ashland Experimental Farm, WI US	S
700	North Raccoon River near Sac City, IA	05482300	Boyer 4 S, IA US	I
762	Nodaway River at Clarinda, IA	06817000	Wallin 1 N, IA US	S
844	Boone River near Webster City, IA	05481000	Webster City, IA US	S
857	Manistee River near Sherman, MI	04124000	Traverse City, MI US	*
966	Oconto River near Oconto, WI	04071765	Peshtigo, WI US	S

1018	Manistee River near Mesick, MI	04124200	Traverse City, MI US	*
1042	River Raisin near Monroe, MI	04176500	Ypsilanti E Michigan University, MI US	I
1080	Peshtigo River at Peshtigo, WI	04069500	Peshtigo, WI US	S
1108	Au Sable River near Red Oak, MI	04136000	Grayling, MI US	I
1340	Ontonagon River near Rockland, MI	04040000	Ontonagon, MI US	S
1361	Au Sable River at Mio, MI	04136500	Glennie 2 SE, MI US	S
1451	Manistee River near Wellston, MI	04125550	Scottville 2 SE, MI US	S
1513	Au Sable River near Mc Kinley, MI	04136900	Glennie 2 SE, MI Us	S
1545	Turkey River at Garber, IA	05412500	Strawberry Point, IA US	S
1547	Cedar River at Waverly, IA	05458300	Shell Rock 2 W, IA US	I
1598	Au Sable River near Curtisville, MI	04137005	Glennie 2 SE, MI US	S
1619	North Raccoon River near Jefferson, IA	05482500	Dexter, IA US	I
1739	Au Sable River near Au Sable, MI	04137500	Glennie 2 SE, MI US	S
1950	Kalamazoo River at New Richmond, MI	04108660	Grand Haven Wastewater Plant, MI US	I
2313	Muskegon River near Croton, MI	04121970	Kent City 2 SW, MI US	I
3441	Raccoon River at Van Meter, IA	05484500	Dexter, IA US	I
5290	Grand River near Eastmanville, MI	04119400	Grand Haven Wastewater Plant, MI US	S
6060	Saginaw River at Holland Avenue At Saginaw, MI	04157005	Vassar, MI US	S
6342	Cedar River at Blairs Ferry Road At Palo, IA	05464420	Central City, IA US	S

12500	Iowa River at Wapello, IA	05465500	Washington, IA US	I
85600	Mississippi River at Clinton, IA	05420500	Bellevue L And D 12, IA US	I
316200	Missouri River at Decatur, NE	06601200	Hornick 5 S, IA US	**

* 95TH Percentile of precipitation intensity was equal to the lowest increment of measurement available

** Mean dT/dt for moderate-intensity days was the equal to the mean dT/dt for high-intensity days

A2. Summary of Water Temperature Regulations for Coldwater Fisheries

Federal

33 U.S. Code, Chapter 26 – Water Pollution Prevention and Control
(33 U.S.C. 26)

- National goal to achieve and maintain a level of water quality which provides for the protection and propagation of fish, shellfish, and wildlife
- Congress shall recognize, preserve, and protect the primary responsibilities and rights of the States to prevent, reduce, and eliminate pollution
- EPA provides assistance to states to establish and implement ongoing water pollution control programs

Iowa

Iowa Administrative Code, Chapter 61 – Water Quality Standards
(567-61.3(455B) Surface water quality criteria., IA ADC 567-61.3(455B))
For coldwater fisheries:

- No increase more than 2°C
- Rate of temperature change cannot exceed 1°C/hr
- Cannot raise temperature above 20°C

Wisconsin

Wisconsin Administrative Code, Chapter NR 102 – Water Quality Standards for Wisconsin Surface Waters
(Wis. Admin. Code NR § 102.25)
For coldwater fisheries:
Maximum allowable weekly average temperatures in °F:

J	F	M	A	M	J	J	A	S	O	N	D
47	47	51	57	63	67	67	65	57	53	48	47

Maximum allowable daily temperatures in °F:

J	F	M	A	M	J	J	A	S	O	N	D
68	68	69	70	72	72	73	73	72	70	69	69

Michigan

Michigan Administrative Code
Water Resources Protection – Part 4. Water Quality Standards
(Mich. Admin. Code R. 323.1075)
For coldwater fisheries:

- May not increase the temperature of the receiving waters at the edge of the mixing zone more than 2°F above the existing natural water temperatures
- May not increase the temperature of the receiving waters at the edge of the mixing zone to temperatures greater than the following monthly maximum temperatures in °F:

J	F	M	A	M	J	J	A	S	O	N	D
38	38	43	54	65	68	68	68	63	56	48	40